Smart Structures and Systems, *Vol. 16, No. 4 (2015) 725-742*
DOI: http://dx.doi.org/10.12989/sss.2015.16.4.725

Performance of TMDs on nonlinear structures subjected to near-fault earthquakes

Martín Domizio[1,2], Daniel Ambrosini*[1,2] and Oscar Curadelli[1,2]

[1]Structural Engineering Master Program. Engineering Faculty, National University of Cuyo, Mendoza, Argentina
[2]CONICET, National Research Council from Argentina, Argentina

(Received October 24, 2014, Revised May 8, 2015, Accepted May 13, 2015)

Abstract. Tuned mass dampers (TMD) are devices employed in vibration control since the beginning of the twentieth century. However, their implementation for controlling the seismic response in civil structures is more recent. While the efficiency of TMD on structures under far-field earthquakes has been demonstrated, the convenience of its employment against near-fault earthquakes is still under discussion. In this context, the study of this type of device is raised, not as an alternative to the seismic isolation, which is clearly a better choice for new buildings, but rather as an improvement in the structural safety of existing buildings. Seismic records with an impulsive character have been registered in the vicinity of faults that cause seismic events. In this paper, the ability of TMD to control the response of structures that experience inelastic deformations and eventually reach collapse subject to the action of such earthquakes is studied.
The results of a series of nonlinear dynamic analyses are presented. These analyses are performed on a numerical model of a structure under the action of near-fault earthquakes. The structure analyzed in this study is a steel frame which behaves as a single degree of freedom (SDOF) system. TMD with different mass values are added on the numerical model of the structure, and the TMD performance is evaluated by comparing the response of the structure with and without the control device.

Keywords: tuned mass damper; near fault earthquakes; collapse; non-linear dynamic analyses

1. Introduction

The use of tuned mass dampers (TMD) has relatively recent applications in civil structures. This passive control device has a mass that oscillates due to the motion of the protected structure, absorbing part of the vibrational energy. A common objective in the control of vibration of civil structures is to reduce the response of the first vibration mode. To accomplish this objective the oscillation frequency of the TMD must be close to the fundamental frequency of the structure that is being protected. The original version of the device, proposed by Frahm (1909), showed great effectiveness in controlling the resonant response produced by harmonic loads of long duration. In order to increase the robustness of the device and to make it effective against loads with different frequency content, various alternatives have been proposed. The use of multiple TMD, both in series (Li and Zhu 2006, Zuo 2009) and in parallel (Iwanami and Seto 1984, Igusa and Xu 1994,

*Corresponding author, Professor, E-mail: dambrosini@uncu.edu.ar

http://www.techno-press.org/?journal=sss&subpage=8 ISSN: 1738-1584 (Print), 1738-1991 (Online)

Warnitchai and Hoang 2006, Li and Ni 2007), is one of these alternatives. The tuning frequency and the values assigned to the mass and damping of the TMD define their performance against different load types. Optimal values of these parameters have been the subject of several studies (Warburton 1982, Chang 1999, Lee *et al*. 2006, Nigdeli and Bekdas 2013) according to different objectives (decrease in maximum displacements, story drift, base shear, etc.) and under different kinds of excitation (harmonic, white noise, etc.).

A change in the fundamental frequency of the structure or TMD causes an effect known as detuning, which decreases the effectiveness of TMD in the control of the structural response. One of the most common causes of detuning is a decrease of the fundamental frequency of the main structure due to the damage experienced under extreme loads. Detuning can also be caused by errors that may exist from the misidentification of the fundamental frequency of the structure or in the erroneous assessment of the soil structure interaction. Furthermore, the detuning of the TMD may be produced by a lack of maintenance of the device as variations in the dynamic properties of the structure due to changes in temperature, occupancy loads and changes in the use of the building. The effects of detuning on the TMD performance has been studied by many authors (Rana and Soong 1998, Wang and Lin 2005, Weber and Feltrin 2010) along with attempts to increase the robustness of the device against changes in the fundamental frequency of the structure and of the control device (Marano *et al*. 2010, Zhang *et al*. 2011, Aly 2014). Another possible solution for the detuning problem is the use of a TMD with semi-active control, such as the device studied by Sun *et al*. (2014),which can be tuned in real time based on the information measured of the main structure.

The effectiveness of TMD on structures subjected to seismic action has been analyzed in several studies (Sladek and Klingner 1983, Villaverde 1994, Bernal 1996, Pinkaew *et al*. 2003, Matta and Destefano 2009, Woo *et al.* 2011, Tributsch and Adam 2012). The TMD performance has shown to be dependent on the duration of the seismic action and on the frequency content relative to the frequency of the vibration modes of the structure being protected. Another influential factor in the performance of the device is the nonlinear behavior of the structure against severe earthquakes. The optimal design of the TMD against such actions also been the subject of various studies (Chakraborty and Roy 2011, Miranda 2013).

In particular, seismic actions recorded in the vicinity of faults have shown a short significant duration, providing most of the energy to the structure in a few seconds. The impulsive property of such actions, called near-fault records, raises doubts on the effectiveness of TMD because these devices have such limited time to counteract the vibrations induced by seismic action. The TMD performance on linear structures against numerous near-fault seismic records was studied by Matta (2011). This study concludes that the TMD is more effective when the frequency content of the excitation is close to the fundamental mode of the structure, achieving a reduction in peak values of displacement of up to 25% when a mass ratio of 10% is assigned to TMD. The analytical model of pulse ground motions proposed by He and Agrawal (2008) was used by Matta (2013) to represent near-fault records and to find the optimal values of TMD parameters against this type of load. The results of this optimization showed significantly lower values than the optimum values obtained for harmonic loads. It is worth mentioning that these studies were performed on the assumption of a linear behavior of the structure during seismic activity. Therefore, the effect of the degradation of both stiffness and strength, which happens in real structures during major earthquakes, is not observed. Under the action of near-fault earthquakes, the performance of a TMD with semi-active control was studied by Sun and Nagarajaiah (2014). This semi-active device can adapt its frequency and damping according to the structural response in order to optimize the transfer and dissipation of energy, showing better results than the passive TMD in reducing peak displacement against pulse-like loads. The collapse of a 4-story steel frame with the addition of TMD against near fault earthquakes was studied by Domizio *et al*. (2015b). The results of this study, where material and geometric nonlinearities were taken into account, showed a direct relationship between the performance of the device and the frequency content of the excitation. When compared to the uncontrolled case, an increase of 30% of peak acceleration required to produce the collapse was achieved with the inclusion of a TMD with a mass ratio of 10%. This increase was observed in the case of a near fault record with high frequency content close to the first mode of the structure.

In this paper the utilization of TMD is proposed, not as an alternative to seismic isolation, which is clearly a better choice for new buildings, but rather as an improvement in the structural safety of existing buildings. In this context, TMD performance was studied by performing nonlinear dynamic analyses on a structure that behaves as a SDOF system subjected to the action of a series of near-fault seismic records. In particular, the ability of the TMD to prevent the collapse was investigated. The value of peak ground acceleration (PGA) that produces structural collapse was founded for each seismic record and a comparison was made between the results obtained in cases with and without control.

2. Description of the numerical model and dynamic actions

The numerical model used in this study was built according the scheme of Fig. 1. This model represents the structure used in experimental tests detailed in the work of Domizio *et al.* (2015a). This study also presents the calibration of the numerical model; which is similar to that used in the present work, and its validation with experimental results.

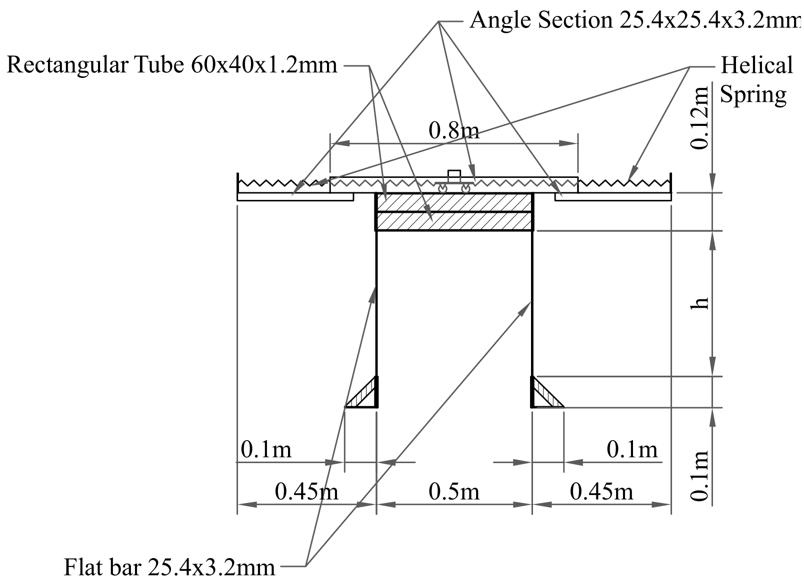

Fig. 1 Scheme of the SDOF structure analyzed

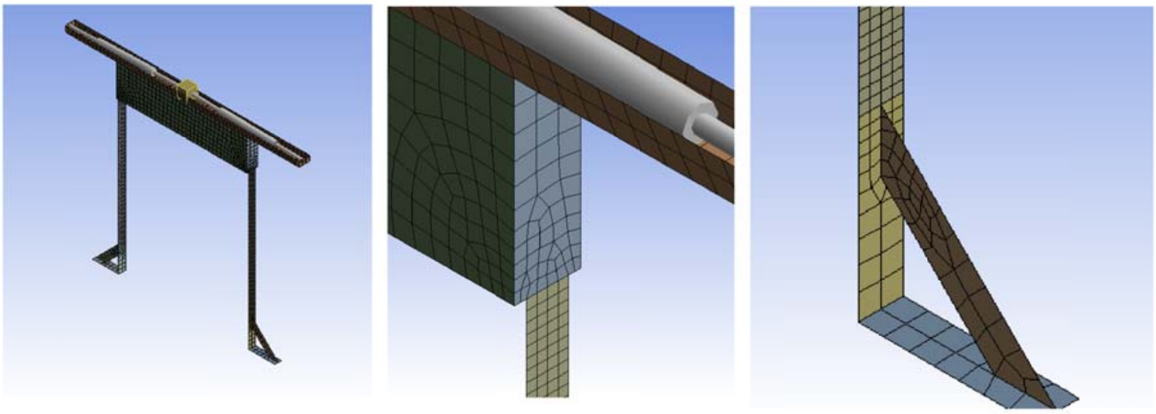

Fig. 2 Mesh of the finite element model

As can be seen in Fig. 1, the columns of the model were made of steel flat bars and the beam was made of a rectangular steel tube filled with lead to achieve the mass values desired. The great bending stiffness of the beam produced a restriction on the rotation of the column ends. This characteristic of the model, together with the large amount of mass concentrated on the beam, causes the behavior of the structure to be dominated by the first vibration mode, acting in an equivalent manner to a SDOF system. In this case a column height of 50 cm and a mass in the beam of 29.5 kg were defined, obtaining a fundamental mode frequency of 1.336 Hz. As already discussed in the work of Domizio *et al*. (2015a), this structure is sensitive to the P-Delta effect due to the combination of the amount of mass concentrated on the beam and the height and stiffness of the columns. As a result of this, the structure reaches dynamic instability and structural collapse under actions with smaller magnitude when compared to structures with less influence of P-Delta effect. In this sense, the mechanism of collapse is substantially different from that of the MDOF structure presented in Domizio *et al*. (2015b)

The TMD of this model comprises a mass that slides on a horizontal guide attached to the beam on the frame structure. The moving mass is connected to the ends of the horizontal guide by a pair of springs, which provides elastic force and centers the mass.

The numerical model of the structure was performed with ANSYS 13 software (ANSYS 2010), using shell finite elements for columns and beams. The type of element selected is suitable for analyses where nonlinear materials are used and where there are large deformations and rotations. Five integration points defined through the thickness for use in plastic range. The mesh of the numerical model was made of squares with a side length of 15mm in the beam and supports, and 6.34 mm in the columns, as can be seen in Fig. 2.

In order to model springs, uniaxial tension-compression elements with two nodes and three degrees of freedom per node were used, defining a viscous damper in parallel with the spring. TMD mass was modeled with an element of one node and six degrees of freedom, in which three values of translational masses and three rotational masses were defined.

The material model was defined as nonlinear steel, with kinematic hardening and a bi-linear stress-strain relationship. An elastic modulus of 208GPa, a yield stress of 360MPa and a strain hardening representing 7.5% of the initial elastic stiffness were defined. Besides the material nonlinearity, geometric nonlinearity was taken into account in the numerical model, due to the large displacements experienced by the structure. The inherent damping assigned to the model is 0.5% of the critical damping, which is close to that estimated in the experimental model from a series of free vibration tests (Domizio 2013).

An example of the capability of the numerical simulation in reproducing the structural collapse is shown in Fig. 3. In this case, the structure was subjected to one of the seismic records used in this study, from the Kobe 1995 earthquake.

The behavior of the TMD is defined by the ratio between the mass of the device and the total mass of the structure, known as mass ratio; by the ratio between the oscillation frequency of the TMD and the fundamental frequency of the structure, known as frequency ratio; and by the damping assigned to the device. Although various authors have studied the performance of TMD on nonlinear structures (Lukkunaprasit and Wanitkorkul 2001, Pinkaew *et al*. 2003, Wong and Johnson 2009, Sgobba and Marano 2010, Woo *et al.* 2011, Lee *et al*. 2012, Mohebbi and Joghataie 2012, Zhang and Balendra 2013), general design formulas for these cases have not been developed. In these previous studies, TMD parameters were determined from numerical optimizations for specific cases or by formulas previously established on assumptions of linear models. In this paper, the frequency ratio and damping of TMD were defined by three expressions. It is noteworthy that the values obtained from these expressions are optimal only for the specific objectives and under the simplifying assumptions with which they were obtained. Two of these expressions were given by Warburton (1982) and they were chosen for this study for having closed forms. These formulas were obtained for a linear SDOF undamped oscillator. In structures with low damping, as these used in this study, the values obtained from these formulas are approximately optimal. The first expression minimizes the main structure displacements when it is subjected to harmonic forces applied at the base. The optimum values of frequency ratio α_{opt} and damping ratio ζ_{opt} of the TMD, in function of the mass ratio μ, are those given by Eqs. (1) and (2).

$$\alpha_{opt} = \frac{\sqrt{1-\frac{\mu}{2}}}{1+\mu} \tag{1}$$

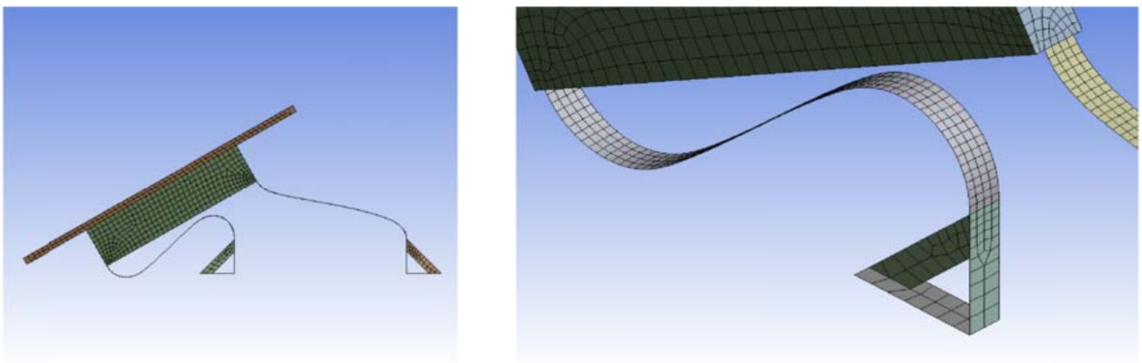

(a) (b)

Fig. 3 Collapse of the structure without TMD. Kobe 1995 record. (a) Front view and (b) Detail of the deformed column

$$\zeta_{opt} = \sqrt{\frac{3\cdot\mu}{8\cdot(1+\mu)\cdot\left(1-\frac{\mu}{2}\right)}} \tag{2}$$

The second expression used to determine the TMD parameters minimizes the RMS value of displacements when white noise excitation acts on the base of the structure. The optimum frequency ratio in this case coincides with the expression 1, while the optimum damping is given by equation 3.

$$\zeta_{opt} = \sqrt{\frac{\mu\cdot\left(1-\frac{\mu}{4}\right)}{4\cdot(1+\mu)\cdot\left(1-\frac{\mu}{2}\right)}} \tag{3}$$

The third expression used in this paper was obtained by Matta (2013) in order to minimize the displacement of the main structure against pulse-like loads. The values of the TMD parameters obtained from this optimization are given by Eqs. (4) and (5).

$$\alpha_{opt} = \frac{\dfrac{\sqrt{1-\frac{\mu}{2}}}{1+\mu}}{1+0.2926\cdot\sqrt{\mu}+\mu^3\cdot\dfrac{0.2301-75.34}{1+30185\cdot\mu^5}} \tag{4}$$

$$\zeta_{opt} = \frac{0.7269\cdot\mu^4-0.3934\cdot\mu^3+0.07388\cdot\mu^2-0.001194\cdot\mu}{\mu^3-0.2978\cdot\mu^2-0.01214\cdot\mu+0.01407} \tag{5}$$

Table 1 summarizes the values of frequency ratio and damping ratio for the three mass ratios and the three optimizations used.

Table 1 Frequency and damping ratio used in the TMD

Mass ratio μ	Optimization for harmonic excitation		Optimization for white noise excitation		Optimization for pulse-like excitation	
	αopt	ζopt	αopt	ζopt	αopt	ζopt
0.010	0.988	0.061	0.988	0.050	0.960	0.000
0.025	0.969	0.096	0.969	0.078	0.927	0.001
0.050	0.940	0.135	0.940	0.110	0.890	0.006

This paper evaluates the performance of TMD against near-fault earthquakes, comparing the response of the structure with and without the implementation of the TMD under a series of 4 seismic records, listed in Table 2. These seismic records have an impulsive character, providing most of the energy to the structure in a few seconds. This is reflected in a short significant duration, defined by Trifunac and Brady (1975) as the time that elapses between 5 and 95% of the Arias intensity. The Arias intensity represents the energy dissipated in the structures due to the seismic action. This measure of intensity was defined by Arias (1970) and can be calculated with equation 6.

$$I_A = \frac{\pi}{2 \cdot g} \cdot \int_0^{t_0} a(t) \cdot dt \tag{6}$$

where g is the gravity acceleration, t_0 is the total earthquake duration, and $a(t)$ is the ground acceleration recorded during an earthquake. The ground acceleration of the seismic records used in this study is shown in Fig. 4, and its significant duration is highlighted.

The response spectrums of the seismic records used in this analysis are shown in Fig. 5. In the figure, the fundamental period of the structure is marked with a continuous line in order to visualize the level of demand on the structure caused by the seismic action. The relationship between the fundamental period of the structure and the dominant frequencies of excitation can also be seen in the figure.

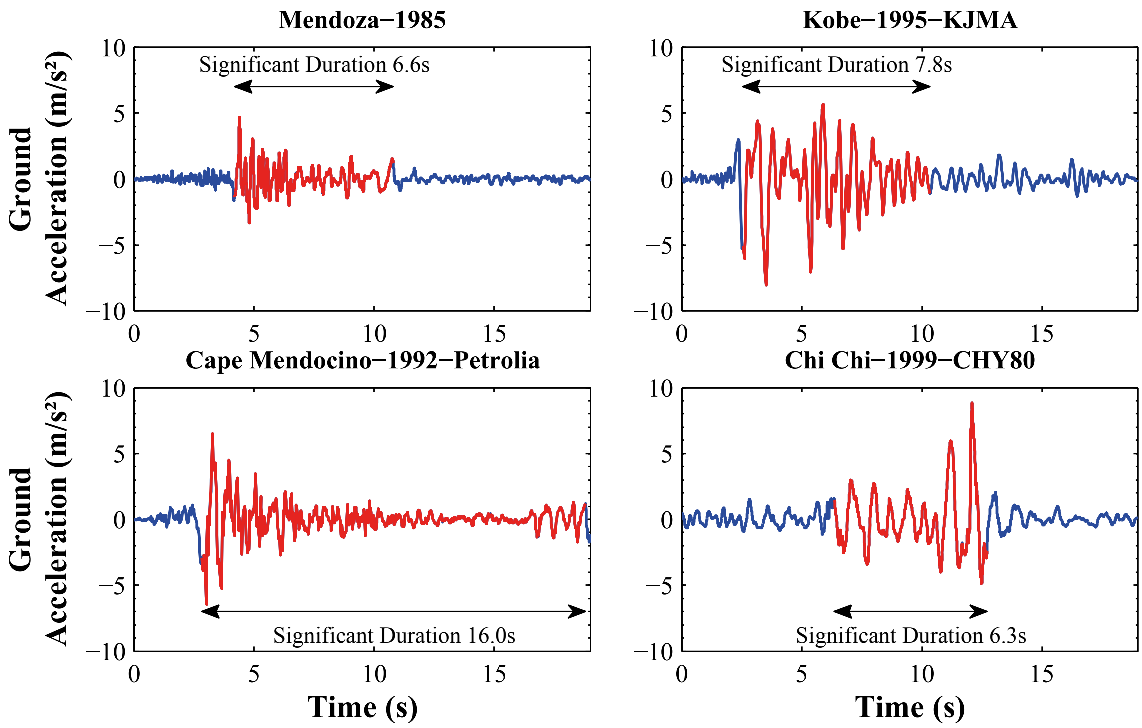

Fig. 4 Acceleration records of the near fault earthquakes

Table 2 Near-fault seismic records used

Event	Year	Moment Magnitude	Station	Distance to rupture plane (km)	Significant Duration (s)	Peak Ground Acceleration (m/s²)
Mendoza, Argentina	1985	6.3	--	--	6.6	4.68
Kobe, Japan (1)	1995	6.9	KJMA	1.0	7.8	8.06
Cape Mendocino, EE.UU (1)	1992	7.0	Petrolia	8.2	16.0	6.50
Chi Chi, Taiwan (1)	1999	7.6	CHY080	2.7	6.3	8.85

(1) Source: PEER Ground Motion Database (http://peer.berkeley.edu)

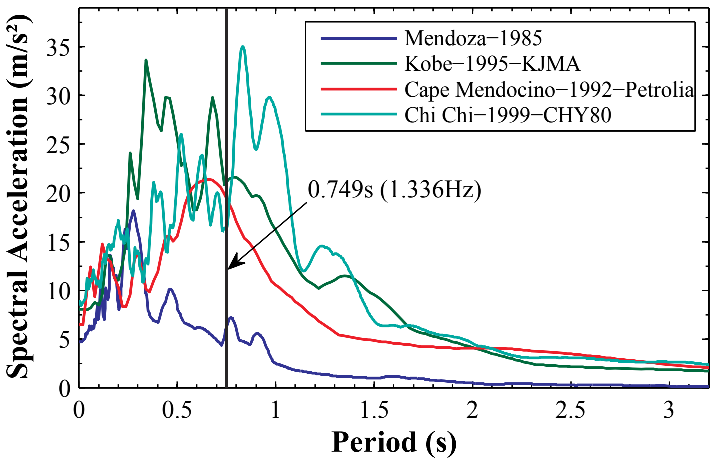

Fig. 5 Response spectrum of the near fault records

3. Analysis with unscaled records

The seismic records used with their original amplitude produce different levels of demand on the structure causing results ranging from an elastic response to structural collapse. The collapse of the structure, without the addition of TMD, occurred in 2 of the 4 cases, as can be seen in Fig. 6, where results in terms of structural displacements are presented. In all cases analyzed, there were no great differences between the responses obtained using the TMD parameters defined by the expression for harmonic and white noise excitation. A lower effectiveness was observed when the formula for the pulse-like excitation was used, likely due to the fact that this expression was obtained from the average characteristics of a particular set of near-fault earthquakes, and not from the specific characteristics of each seismic record used in this study. Fig. 6 also shows that, when Kobe 1995 and Chi Chi 1999 records were used, TMD failed to prevent the collapse of the structure, even when mass ratios of 5% were used. It can also be seen that the use of TMD produces variations in the time when the collapse occurs. However, this change does not become significant, showing that, for this level of demand, the addition of TMD represents no benefit. From Fig. 6, it is also possible to see that TMD has no effect on the structural response during the first half cycle of model´s oscillation. Nonetheless, the device achieved a significant reduction of the inelastic displacements after this initial moment when the Cape Mendocino 1992 earthquake record was employed, and it was able to diminish the peak displacement for the record of the Mendoza 1985 earthquake. The results of the cases where the structure without TMD did not collapse are summarized in Table 3 in terms of structural displacement, acceleration and base shear force.

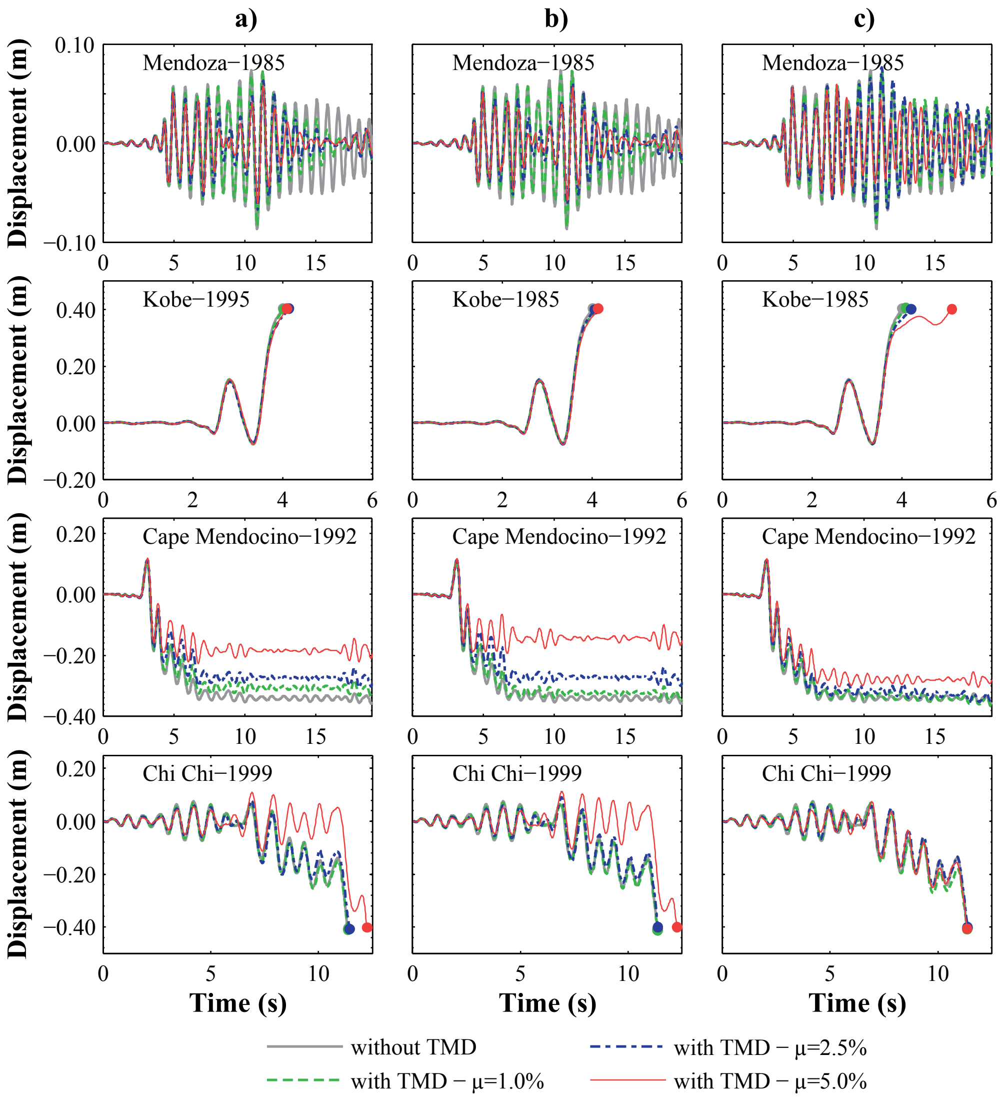

Fig. 6 Displacement of the main structure with TMD parameters optimized for: (a) harmonic excitation, (b) white noise excitation and (c) pulse-like excitation

Table 3 Results in the main structure without TMD

Event	Year	Station	Displacement		Acceleration		Base Shear	
			Max. (m)	RMS (m)	Max. (m/s²)	RMS (m/s²)	Max. (N)	RMS (N)
Mendoza	1985	--	0.086	0.032	6.68	2.24	144.4	66.1
Cape Mendocino	1992	Petrolia	0.362	0.307	7.60	1.34	174.0	35.1

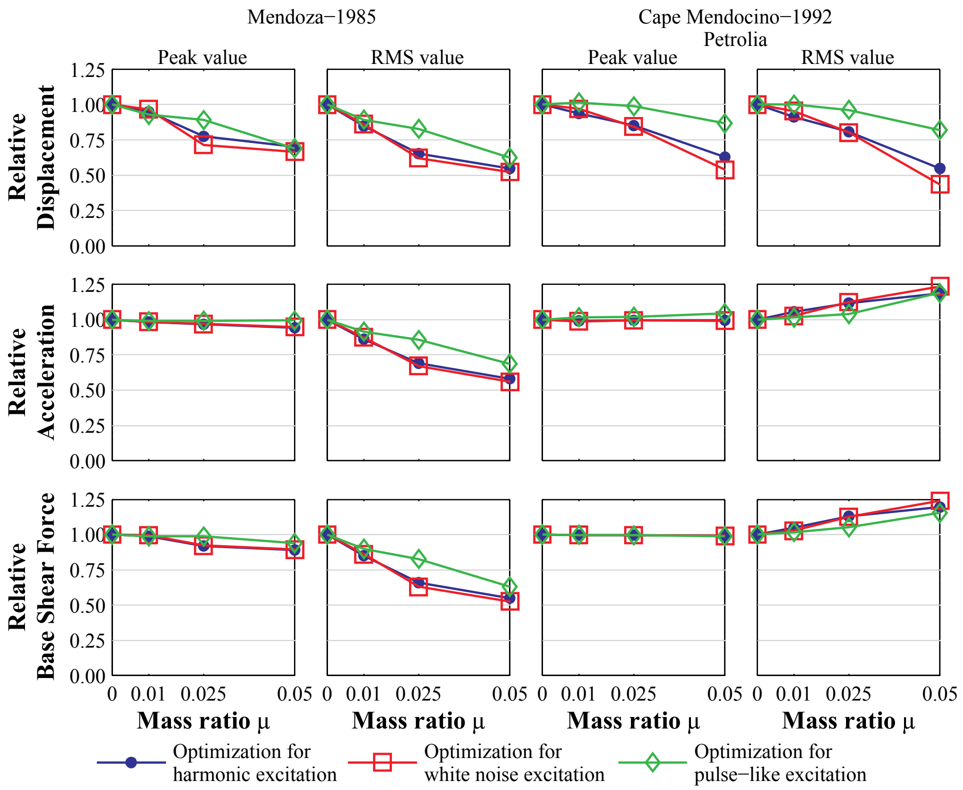

Fig. 7 Response of the main structure with TMD added, relative to uncontrolled case

In Fig. 7, the response of the structure with TMD against the near-fault records of Mendoza 1985 and Cape Mendocino 1992 earthquakes are shown. These responses are expressed here as relative to the results obtained in the case without control. From this figure, it can be seen that the device is more effective in reducing the displacements of the main structure than it is for acceleration and for the base shear force. It can also be observed that the response reduction compared to the uncontrolled case is higher in terms of RMS values than peak values. Once again, similar responses can be observed in cases where TMD parameters were defined for harmonic and white noise excitation.

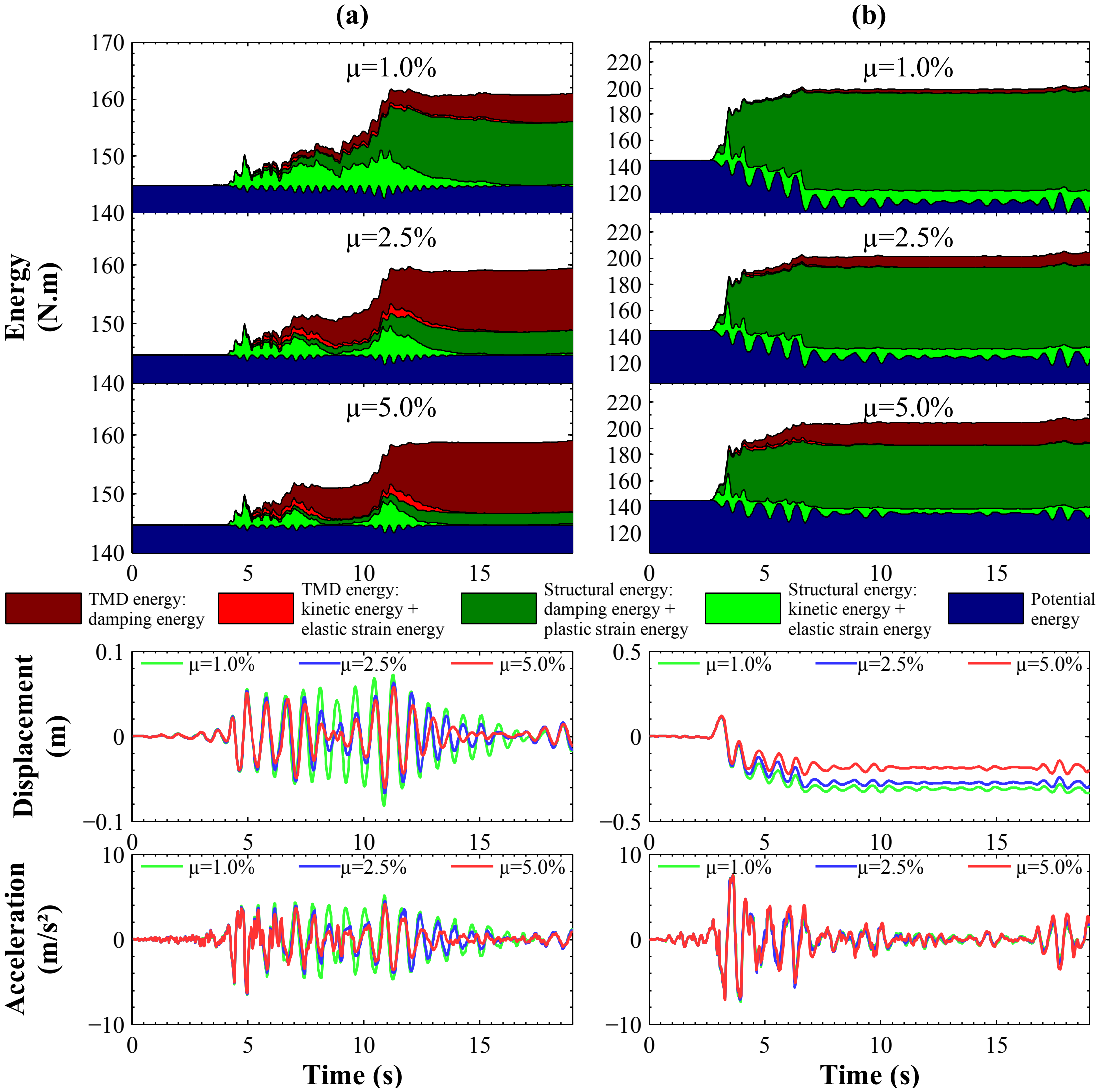

Fig. 8 Energy input, displacement and acceleration of the structure against: (a) Mendoza 1985 earthquake and (b) Cape Mendocino1992 earthquake

In particular, against the action of the Cape Mendocino earthquake, it can be seen how the increase in the TMD mass causes an increase in RMS values for acceleration and for base shear force, but remains unchanged at their peak values. This increase in the RMS values can be explained by observing the displacement of the structure against this seismic record in Fig. 6. In this figure, it can also be seen that an increase in TMD mass ratio decreases the remaining deformation of the structure with the consequent reduction of peak and RMS values in terms of displacements. On the other hand, the displacement amplitude increases around the remaining deformation after the cycle that produces most plastic deformation. Because of this, the RMS values of acceleration and base shear force are larger when compared to the uncontrolled case. Meanwhile, the peak values show no variation in terms of acceleration and base shear force because they occur in the first cycle of the earthquake where the TMD practically has no influence.

Fig. 8 shows variations in time concerning the system energy for the two cases studied without collapse and parameters optimized for harmonic excitation. This energy is the sum of the energy in the structure, the energy in the TMD and the gravitational potential energy of the complete system. Both terms include kinetic energy, strain energy (due to plastic and elastic strain in the structure, and only elastic strain in TMD), and the energy dissipated by damping. The figure also shows the displacement and acceleration of the structure.

In Fig. 8(a) it can be seen that there is no energy transfer to the TMD during the initial pulse of the Mendoza seismic record. However, the device was effective in reducing the maximum displacement of the structure because this occurred in the middle of the strong phase of the ground motion with an energy transfer between the structure and the control device. This transfer of energy increases along with the addition in the mass used in the TMD, as expected. It can also be seen that under this dynamic action, there are no permanent deformations in the structure, and the amount of input energy is mostly dissipated by the device when the mass ratio reaches 5%, unlike the case shown in Fig. 8(b), where the energy dissipated hysterically by inelastic deformations has a greater relative importance. As was mentioned before, against the Cape Mendocino seismic record, the addition of TMD to the structure led to significant reductions in the response from the second half cycle of displacement onward. This benefit increases as the mass value assigned to the device grows, as expected. This behavior is due to the proximity between the fundamental frequency of the structure and the main frequency of the seismic action, as can be deduced from the response spectrum.

4. Collapse acceleration analysis

In the analysis described in the previous section, the effect of TMD on the structural response for each seismic record used with its original amplitude was studied. The purpose of this section is to determine which is the lowest excitation amplitude that produces structural collapse, with and without the incorporation of the TMD and evaluating the benefit obtained by the addition of the device. The bisection method was used in order to find this ground motion amplitude by first searching an adequate amplitude range. Once the initial range was established, the occurrence of the structural collapse was evaluated in each iteration, subdividing the range by half according to the result. In this study, results are presented as a function of peak ground acceleration (PGA), which is the record parameter scaled in each iteration. Table 4 shows an example of the method used, in which the structure without TMD is subjected to the seismic record of the Kobe 1995 earthquake, and the resulting displacements of each iteration are shown in Fig. 9.

The smallest PGAs which produce the collapse, called collapse PGA, of the structure without TMD are presented in Table 5.

Fig. 10 shows the collapse PGA of the four seismic records when the TMD is attached to the main structure with the parameter values defined according to the three expressions mentioned in section 2. These collapse PGAs are given as relative to the results of the case without the implementation of the device.

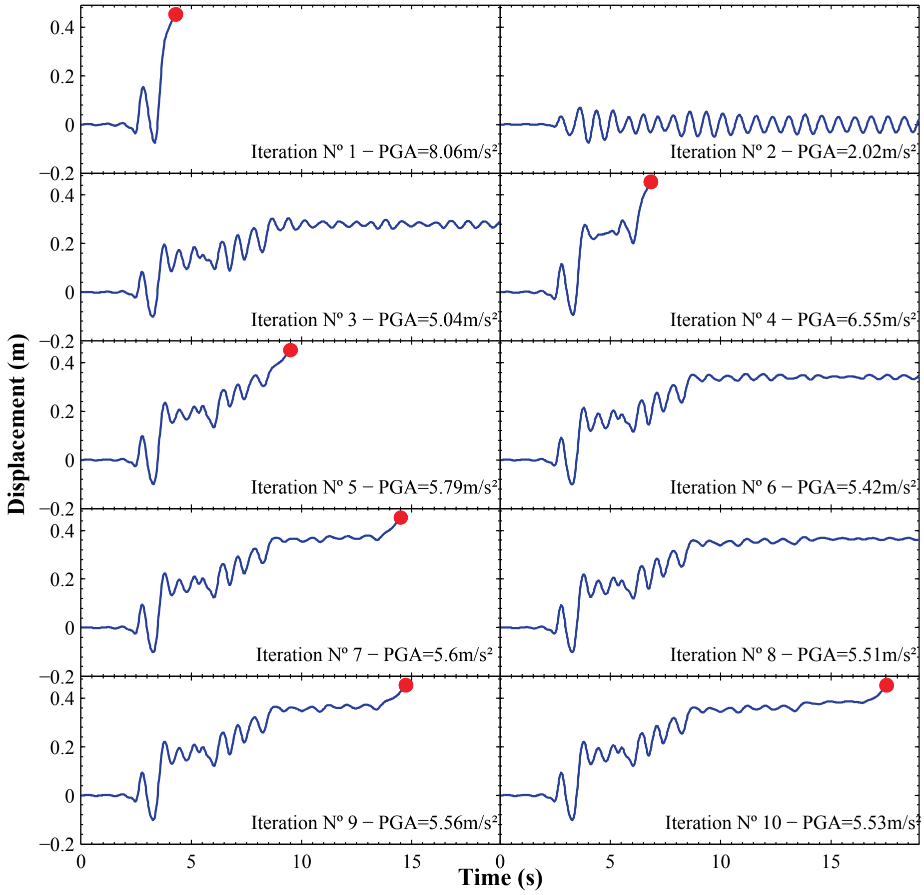

Fig. 9 Displacement of the structure without TMD. Kobe 1995 record

Table 4 Determination of the minimum amplitude of the Kobe 1995 record that cause the collapse of the structure without TMD

Stage	Iteration Number	Peak Ground Acceleration - PGA (m/s^2)			Iteration Result
		Upper Limit w/o Collapse	Lower Limit w/ Collapse	Used in the Current Iteration	
Initial range search	1	---	---	8.06	w/ collapse
	2	---	8.06	2.02	w/o collapse
Range bisection	3	2.02	8.06	5.04	w/o collapse
	4	5.04	8.06	6.55	w/ collapse
	5	5.04	6.55	5.79	w/ collapse
	6	5.04	5.79	5.42	w/o collapse
	7	5.42	5.79	5.60	w/ collapse
	8	5.42	5.60	5.51	w/o collapse
	9	5.51	5.60	5.56	w/ collapse
	10	5.51	5.56	5.53	w/ collapse

Table 5 Collapse PGA of the structure without TMD

Event	Year	Station	Collapse PGA (m/s²)
Mendoza,	1985	--	13.95
Kobe, Japan	1995	KJMA	5.53
Cape Mendocino	1992	Petrolia	7.42
Chi Chi	1999	CHY080	5.01

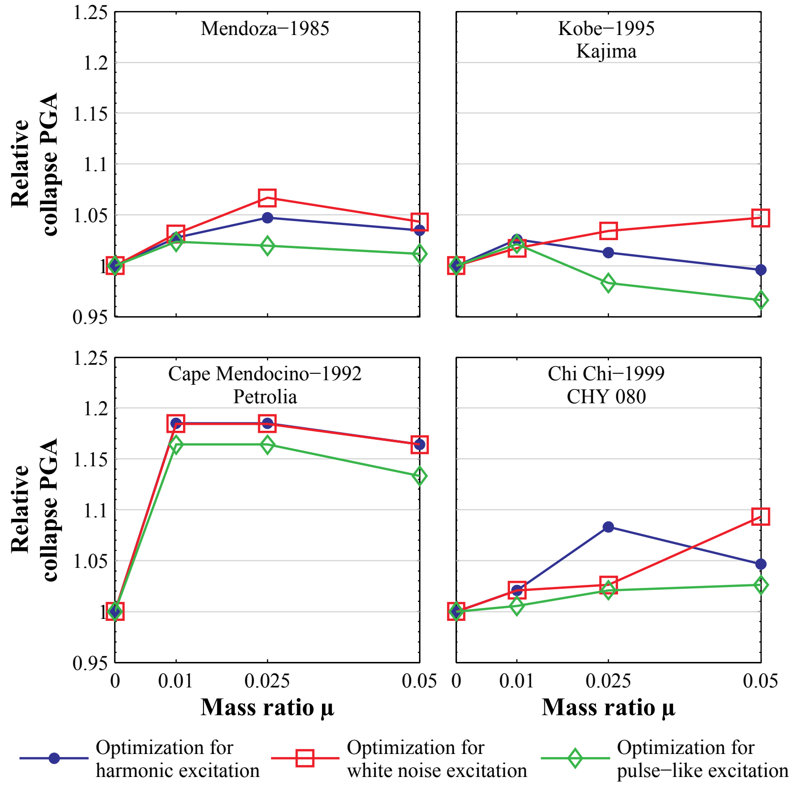

Fig. 10 Collapse PGA of the structure with TMD, relative to the uncontrolled case

As it can be seen in Fig. 10, in most cases where the TMD is incorporated, the acceleration necessary to produce the collapse was higher when compared to the acceleration required for the structural collapse in the uncontrolled case. However, there is a relatively large dispersion in the benefit obtained by the addition of the device, with limits between -3 and 19%. Under the action of the same seismic record and with the same amount of mass assigned to the device, the results showed dispersion in the TMD performance due to the different criteria used in defining their damping and tuning frequency. These results show a higher response sensitivity to the value adopted in TMD parameters when compared to the results obtained from the analysis of the previous section under unscaled records. In this case, the optimization for white noise excitation showed the best performance in most cases and the largest increase in the collapse PGA was obtained for the Cape Mendocino seismic record, which is the ground motion that has the dominant frequencies closest to the frequency of the fundamental mode of the structure. Moreover, if the most common value of mass of TMD of 1% is used, the three optimization methods give similar results.

In the study performed on a MDOF structure by Domizio *et al.* (2015b), the use of higher mass ratios resulted in higher collapse PGA for all cases where the inclusion of the TMD was effective. However, from the results of the present study over an equivalent SDOF, it can be seen that a larger benefit does not always occur with an increase of mass in the TMD. It is clear in the case of this study that the most convenient mass value for the TMD is between 1 and 2.5%, which is a significant result.

Fig. 11 shows the results obtained in the structure with a TMD mass ratio of 2.5% and 5% in order to understand why an increase in the TMD mass can lead to a decrease in the collapse acceleration.

This figure shows the displacement of the structure subjected to Chi-Chi earthquake scaled to the collapse PGA and TMD parameters defined according to the expression for harmonic excitation. The total force exerted by the TMD on the structure (sum of the force exerted by the spring and by the viscous damper of the device), and the energy transfer rate between the structure and TMD, obtained as the product of the TMD force by velocity of the structure, are also shown. When the force exerted by the TMD and the velocity of the structure have opposite directions, the control device absorbs energy. However, in the case in which the greater mass ratio (μ=5%) was used, it can be seen how a relatively large amount of energy returns from the device at the moment when the structure undergoes the largest inelastic deformations. Furthermore, at this same time, the TMD exerts force in the same direction in which collapse finally occurs. Due to this the dynamic instability is reached more easily, especially in structures with high influence of the P-Delta effect, such as those used in this study.

5. Conclusions

In this paper the TMD performance on a SDOF structure subject to a series of near-fault earthquakes was studied. With this aim two different analyses were performed, defining the TMD parameters according to expressions of optimal values for harmonic, white noise and pulse-like excitation. In the first analysis, 4 unscaled near-fault records were used, noting that, in cases where the structure did not collapse, a TMD with a mass ratio of 5% was able to reduce the RMS displacement values up to 50% and peak values up to 45%. Peak values could be reduced because these did not take place in the first half cycle of oscillation, in which the device has no effect on the structural response, being unable to absorb energy from the structure. However, from the second half cycle of oscillation a significant decrease of inelastic deformations was observed when the record of Cape Mendocino earthquake was used as input. The device efficiency in controlling accelerations and the base shear force was significantly lower. In cases when the uncontrolled structure collapsed, TMD implementation was not effective to prevent it because the level of demand was too high to be beneficial. Similar results were obtained when the TMD parameters defined for harmonic and white noise excitation were employed, and less effectiveness was observed when the expression obtained for pulse-like loads was used.

In the second analysis, the amplitudes of the four near-fault records that produce structural collapse were found. From the results of this analysis, it was observed that the incorporation of TMD allowed the collapse PGA to increase up to 19% in the case where the action has frequency content near to the fundamental mode frequency of the structure reaching up to 9% in the other cases. It was also observed that the major benefits were obtained with mass ratios values between 1% and 2.5%, with a decrease of these benefits in some cases when the mass ratio of 5% was used. In one case, where the increase in the mass ratio reduced the collapse PGA, a relatively large energy return from the TMD to the structure was observed. The force exerted by the device on the structure at that time had the same direction of collapse, which may favor the dynamic instability of structures with high influence of the P-Delta effect, such as analyzed in this study. In this case, the optimization for white noise excitation showed the best performance in most cases and if the most common value of mass of TMD of 1% is used, the three optimization methods give similar results.

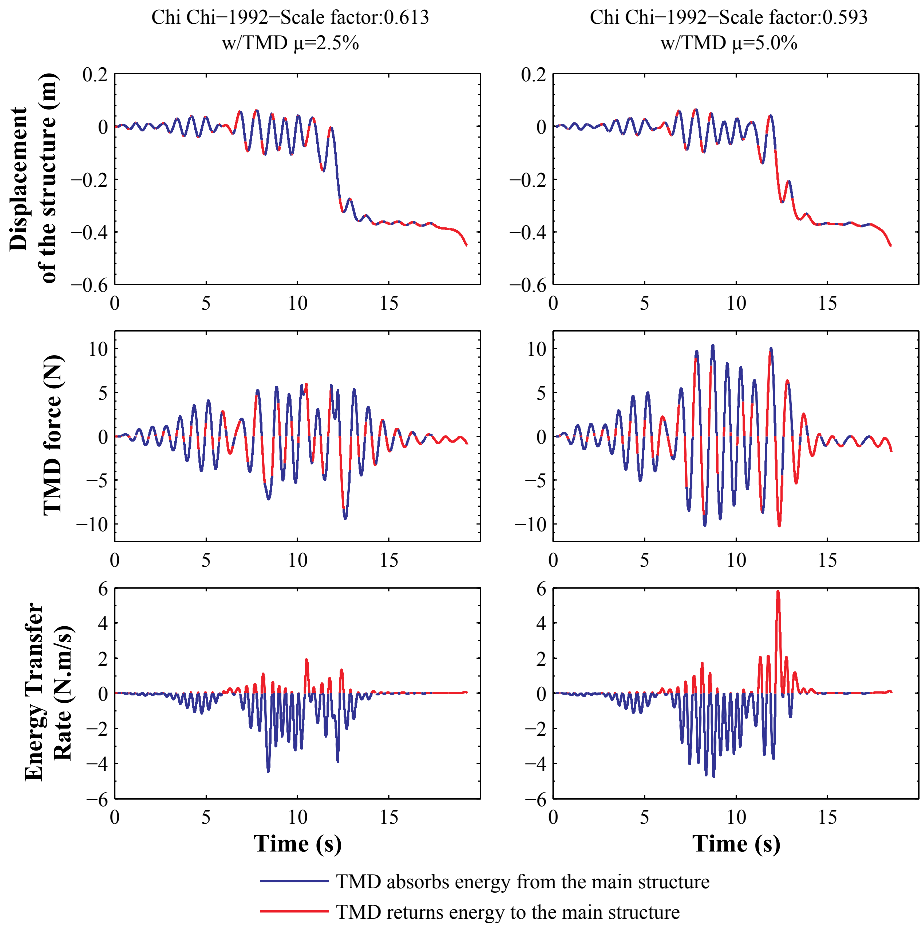

Fig. 11 Response of the structure with TMD mass ratios of 2.5% and 5% against Chi-Chi seismic record scaled to the collapse PGA

Acknowledgments

The financial support of CONICET and the National University of Cuyo is gratefully acknowledged. Special acknowledgements are extended to the reviewers of the first version of the paper because their useful suggestions led to improvements of the work.

References

Aly, A.M. (2014), “Vibration control of high-rise buildings for wind: a robust passive and active tuned mass damper”, *Smart Struct. Syst.*, **13**(3), 473-500.
ANSYS, I. (2010), *Theory reference*, Canonsburg: ANSYS, Inc.
Arias, A. (1970), “A measure of earthquake intensity”, In: *Seismic Design for Nuclear Power Plants*. (Ed. R.J. Hansen), Massachusetts Inst. of Tech. Press, Cambridge, MA.
Bernal, D. (1996), “Influence of ground motion characteristics on the effectiveness of tuned mass dampers”, *Proceedings of the 11th World Conference on Earthquake Engineering*. Acapulco, Mexico, June.
Chakraborty, S. and Roy, B.K. (2011), “Reliability based optimum design of tuned mass damper in seismic vibration control of structures with bounded uncertain parameters”, *Probabilist. Eng. Mech.*, **26**(2), 215-221.
Chang, C.C. (1999), “Mass dampers and their optimal designs for building vibration control”, *Eng. Struct.*, **21**(5), 454-463.
Domizio, M., Ambrosini, D. and Curadelli, O. (2015a), “Experimental and numerical analysis to collapse of a framed structure subjected to seismic loading”, *Eng. Struct.*, **82**, 22-32.
Domizio, M., Ambrosini, D. and Curadelli, O. (2015b), “Performance of tuned mass damper against structural collapse due to near fault earthquakes”, *J. Sound Vib.*, **336**, 32-45.
Domizio, M.N. (2013), *Análisis numérico y experimental del desempeño de amortiguadores de masa sintonizada frente a sismos de falla cercana*, M.Eng. Dissertation, National University of Cuyo, Mendoza, Argentina.
Frahm, H. (1909), *Device for damped vibrations of bodies*, US patent No. 989958.
He, W. and Agrawal, A.K. (2008), “Analytical model of ground motion pulses for the design”, *J. Struct. Eng. - ASCE*, **134**(7), 1177-1188.
Igusa, T. and Xu, K. (1994), “Vibration control using multiple tuned mass dampers”, *J. Sound Vib.*, **175**(4), 491-503.
Iwanami, K. and Seto, K. (1984), “An optimum design method for the dual dynamic damper and its effectiveness”, *Bull. JSME*, **27**, 1965-1973.
Lee, C., Chen, Y., Chung, L. and Wang, Y. (2006), “Optimal design theories and applications of tuned mass dampers”, *Eng. Struct.*, **28**(1), 43-53.
Lee, C.S., Goda, K. and Hong, H.P. (2012), “Effectiveness of using tuned-mass dampers in reducing seismic risk”, *Struct. Infraestruct. E.*, **8**(2), 141-156.
Li, C. and Zhu, B. (2006), “Estimating double tuned mass dampers for structures under ground acceleration using a novel optimum criterion”, *J. Sound Vib.*, **298**(1-2), 280-297.
Li, H.N. and Ni, X.L. (2007), “Optimization of non-uniformly distributed multiple tuned mass damper”, *J. Sound Vib.*, **308**(1-2), 80-97.
Lukkunaprasit, P. and Wanitkorkul, A. (2001), “Inelastic buildings with tuned mass dampers under moderate ground motions from distant earthquakes”, *Earthq. Eng. Struct. D.*, **30**(4), 537-551.
Marano, G.C., Greco, R. and Sgobba, S. (2010), “A comparison between different robust optimum design approaches: application to tuned mass dampers”, *Probabilist. Eng. Mech.*, **25**(1), 108-118.
Matta, E. (2013), “Effectiveness of tuned mass dampers against ground motion pulses”, *J. Struct. Eng.- ASCE*, **139**(2), 188-198.

Matta, E. (2011), "Performance of tuned mass dampers against near-field earthquakes", *Struct. Eng. Mech.*, **39**(5), 621-642.
Matta, E. and Destefano, A. (2009), "Seismic performance of pendulum and translational roof-garden tmds", *Mech. Syst. Signal Pr.*, **23**(3), 908-921.
Miranda, J.C. (2013), "A method for tuning tuned mass dampers for seismic applications", *Earthq. Eng. Struct. D.*, **42**(7), 1103-1110.
Mohebbi, M. and Joghataie, A. (2012), "Designing optimal tuned mass dampers for nonlinear frames by distributed genetic algorithms", *Struct. Des. Tall Spec.*, **2**1(1), 57-76.
Nigdeli, S.M. and Bekdas, G. (2013), "Optimum tuned mass damper design for preventing brittle fracture of rc buildings", *Smart Struct. Syst.*, **12**(2), 137-155.
Pinkaew, T., Lukkunaprasit, P. and Chatupote, P. (2003), "Seismic effectiveness of tuned mass dampers for damage reduction of structures", *Eng. Struct.*, **25**(1), 39-46.
Rana, R. and Soong, T.T. (1998), "Parametric study and simplified design of tuned mass dampers", *Eng. Struct.*, **20**(3), 193-204.
Sgobba, S. and Marano, G.C. (2010), "Optimum design of linear tuned mass dampers for structures with nonlinear behaviour", *Mech. Syst. Signal Pr.*, **24**(6), 1739-1755.
Sladek, J.R. and Klingner, R.E. (1983), "Effect of tuned mass dampers on seismic response", *J. Struct. Eng. - ASCE*, **109**(8), 2004-2009.
Sun, C. and Nagarajaiah, S. (2014), "Study on semi-active tuned mass damper with variable damping and stiffness under seismic excitations", *Struct. Control Heal. Monit.*, **21**(6), 890-906.
Sun, C., Nagarajaiah, S. and Dick, A.J. (2014), "Family of smart tuned mass dampers with variable frequency under harmonic excitations and ground motions: closed-form evaluationde la estructura", *Smart Struct. Syst.*, **13**(2), 319-341.
Tributsch, A. and Adam, C. (2012), "Evaluation and analytical approximation of tuned mass damper performance in an earthquake environment", *Smart Struct. Syst.*, **10**(2), 155-179.
Trifunac, M. and Brady, A.G. (1975), "A study on the duration of strong earthquake ground motion", *B. Seismol. Soc. Am.*, **65**(3), 581-626.
Villaverde, R. (1994), "Seismic control of structures with damped resonant appendages", *Proceedings of the 1st World Conference on Structural Control*, Vol. 1. Los Angeles, USA, August.
Wang, J. and Lin, C. (2005), "Seismic performance of multiple tuned mass dampers for soil–irregular building interaction systems", *Int. J. Solids Struct.*, **42**(20), 5536-5554.
Warburton, G.B. (1982), "Optimal absorber parameters for various combinations of response and excitation parameters", *Earthq. Eng. Struct. D.*, **10**(3), 381-402.
Warnitchai, P. and Hoang, N. (2006), "Optimal placement and tuning of multiple tuned mass dampers for suppressing multi-mode structural response", *Smart Struct. Syst.*, **2**(1), 1-24.
Weber, B. and Feltrin, G. (2010), "Assessment of long-term behavior of tuned mass dampers by system identification", *Eng. Struct.*, **32**(11), 3670-3682.
Wong, K.K.F. and Johnson, J. (2009), "Seismic energy dissipation of inelastic structures with multiple tuned mass dampers", *J. Eng. Mech.- ASCE*, **135**(4), 265-276.
Woo, S.S., Lee, S.H. and Chung, L. (2011), "Seismic response control of elastic and inelastic structures by using passive and semi-active tuned mass dampers", *Smart Struct. Syst.*, **8**(3), 239-252.
Zhang, H., Shi, Y. and Saadat, A. (2011), "Robust non-fragile dynamic vibration absorbers with uncertain factors", *J. Sound Vib.*, **330**(4), 559-566.
Zhang, Z. and Balendra, T. (2013), "Passive control of bilinear hysteretic structures by tuned mass damper for narrow band seismic motions", *Eng. Struct.*, **54**, 103-111.
Zuo, L. (2009), "Effective and robust vibration control using series multiple tuned-mass dampers", *J. Vib. Acoust.*, **131**, 031003.

BS